

## Generation of Point Defects in Crystalline Silicon by MeV Heavy Ions: Dose Rate and Temperature Dependence

B. G. Svensson,\* C. Jagadish, and J. S. Williams

*Department of Electronic Materials Engineering, Research School of Physical Sciences and Engineering,  
The Australian National University, Canberra, Australian Capital Territory 0200, Australia*

(Received 9 April 1993)

Si(100) samples have been implanted with low doses ( $10^7$ – $10^9$  cm $^{-2}$ ) of MeV  $^{76}\text{Ge}$  and  $^{120}\text{Sn}$  ions. Deep level transient spectroscopy was used for sample analysis, and the generation of vacancy-related point defects is found to *increase with increasing implantation temperature* and to *decrease with increasing ion dose rate*. These results are in direct contrast to that for damage buildup at high doses ( $\geq 10^{12}$  cm $^{-2}$ ), and the effect is attributed to rapidly diffusing Si self-interstitials which overlap and annihilate vacancies created in adjacent ion tracks.

PACS numbers: 61.72.Bb, 61.72.Tt, 61.80.Jh, 71.55.Ht

Implantation of energetic ions into crystalline semiconductors gives rise to atomic displacements and structural defects. The generation of stable defects depends on several parameters, e.g., ion energy, ion mass, sample temperature, ion dose, and dose rate. A process of crucial importance for damage buildup in semiconductors is defect annealing during implantation [1–4]. Usually, one distinguishes between two types of annealing processes during ion implantation [5]: (i) thermal or bulk annealing and (ii) dynamic annealing. Type (i) resembles ordinary thermal annealing and is caused by a rise in target temperature during high dose rate ion bombardment. In the following, we will concentrate on type (ii), and in particular, its dependence on dose rate and sample temperature.

For doses above  $\sim 10^{12}$  cm $^{-2}$  and dose rates in the range of  $\sim 10^{11}$  to  $10^{15}$  cm $^{-2}$ s $^{-1}$  it is well established that the influence of dynamic annealing in semiconductors decreases with increasing dose rate and decreasing target temperature [1–6]. Alternative explanations exist for these effects [5,6] and one among others is that at sufficiently high dose rates, collision cascades can overlap before the single cascade defects have completed their annealing process [5]. As a result, a higher concentration of defects which are more stable at (and above) room temperature (RT) is formed. At low enough target temperatures the mobility of migrating defects responsible for the annealing process decreases, and the ion-induced damage is to a large extent “frozen in” [4]. Again, a high concentration of stable defects is generated in the single cascades as dynamic annealing diminishes.

Recently, Hallén *et al.* [7] irradiated silicon at RT with 1.3 MeV protons using a dose of only  $5 \times 10^9$  cm $^{-2}$  and dose rates of  $10^7$  to  $10^{10}$  cm $^{-2}$ s $^{-1}$ . In direct contrast to the results for heavier ions and higher doses and dose rates, they found a reverse dose rate dependence; i.e., for a constant dose the resulting defect density decreased with increasing dose rate.

In this work silicon samples have been implanted with low doses of MeV  $^{76}\text{Ge}$  and  $^{120}\text{Sn}$  ions using different

dose rates and sample temperatures. To the best of our knowledge, we have observed for the first time a “reverse” temperature and dose rate dependence for point defect production by heavy ions in silicon. Indeed, the generation rate of divacancy centers ( $V_2$ ) is reduced by a factor of  $\sim 2$  as the implantation temperature decreases from  $\sim 300$  to 100 K and by a factor of  $\sim 2.5$  as the dose rate increases from  $\sim 10^7$  to  $10^9$  cm $^{-2}$ s $^{-1}$ .

Czochralski-grown (Cz) and phosphorus-doped *n*-type (0.4 and 0.6  $\Omega$  cm) Si(100) samples were implanted with  $^{76}\text{Ge}$  and  $^{120}\text{Sn}$  ions to doses in the range  $5 \times 10^7$  and  $1.2 \times 10^9$  cm $^{-2}$  using the 1.7 MV NEC Tandem implanter at our laboratory. Energies between 1.0 and 8.0 MeV were used, and the ion beam was scanned over an aperture ( $2.5 \times 4$  cm $^2$ ) to ensure uniformity (horizontal scan rate 517 Hz and vertical scan rate 64 Hz). The average dose rate and sample temperature during implantation were varied from  $1.5 \times 10^7$  to  $6 \times 10^8$  cm $^{-2}$ s $^{-1}$  and 95 to 304 K, respectively. Careful attention was given to accurate dosimetry at the low doses used. Under the highest dose rate conditions used the error in nominal dose never exceeded 20%. After implantation, the samples were chemically cleaned using a standard procedure which included a final dip in diluted hydrofluoric acid. Immediately after cleaning, the samples were loaded into a vacuum chamber where Schottky barrier contacts were formed by thermal evaporation of gold at a base pressure of  $2 \times 10^{-6}$  Torr. In order to avoid annealing effects the sample temperature never exceeded 40°C during the evaporation. Deep level transient spectroscopy (DLTS) was applied for sample analysis; the setup used is a refined version of the one described in Ref. [8]. The steady-state reverse bias and pulse voltages during the DLTS measurements were such that the entire defect distribution was monitored. The length of time between diode fabrication and DLTS measurement was normally less than 48 h and in some cases only 2 h. No influence of this delay time has been observed in the range of 2 h to 6 months.

Figure 1 shows two DLTS spectra obtained after im-

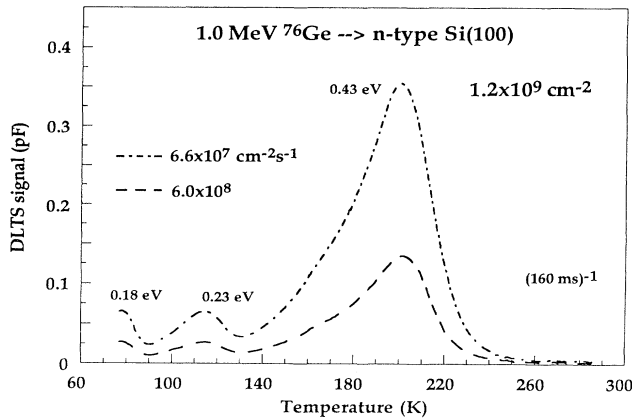


FIG. 1. DLTS spectra of two *n*-type Si(100) samples implanted with 1.0 MeV  $^{76}\text{Ge}$  ions to a dose of  $1.2 \times 10^9 \text{ cm}^{-2}$  using dose rates of  $6.6 \times 10^7$  and  $6.0 \times 10^8 \text{ cm}^{-2}\text{s}^{-1}$ . The reverse bias and plus voltages were 11 and 10.5 V, respectively.

plantation of 1.0 MeV  $^{76}\text{Ge}$  ions with dose rates of  $6.6 \times 10^7$  and  $6.0 \times 10^8 \text{ cm}^{-2}\text{s}^{-1}$ . The dose is kept constant at  $1.2 \times 10^9 \text{ cm}^{-2}$  but the peak amplitudes are lower by a factor of  $\sim 2.5$  for the high dose rate. Three levels are clearly resolved in both spectra; they appear at  $\sim 0.18$ ,  $\sim 0.23$ , and  $\sim 0.43$  eV below the conduction band edge ( $E_c$ ). The  $E_c - 0.18$  eV level is well known and is due to the vacancy-oxygen center (VO or the *A* center) [9]. The levels at  $E_c - 0.23$  and  $E_c - 0.43$  eV are normally associated with the doubly and singly negative charge state of  $V_2$ , respectively [10–13]. In highly doped Cz ( $\ll 1 \Omega \text{ cm}$ ) and moderately doped float zone ( $\leq 10 \Omega \text{ cm}$ ) materials the latter level is substantially influenced by the overlapping signal from the vacancy-phosphorus center (VP or the *E* center) [11,12]. According to our earlier annealing results, the contribution from VP to the  $E_c - 0.43$  eV peak is found to be  $< 20\%$  in the materials used in the present study [14]. On the low-temperature shoulder of the  $E_c - 0.43$  eV peak, a broad tail appears, and more detailed studies using B- and Si-implanted samples reveal an overlapping peak which occurs  $\sim 0.35$  eV below  $E_c$  [14].

In Fig. 2 the amplitude of the peaks at  $E_c - 0.23$  and  $E_c - 0.43$  eV is plotted as a function of dose rate for 1.0 MeV  $^{76}\text{Ge}$  and 2.3 MeV  $^{120}\text{Sn}$  ions, keeping the dose constant at  $1.2 \times 10^9$  and  $6 \times 10^8 \text{ cm}^{-2}$ , respectively. A substantial decrease in the peak amplitudes is observed above  $\sim 10^8 \text{ cm}^{-2}\text{s}^{-1}$ . Except for a shift in absolute values by somewhat more than 1 order of magnitude, this dependence is similar to that observed for protons [7], despite the fact that the density of elastic energy deposition per ion per  $\text{\AA}$  differs by 3 orders of magnitude. This indicates that the magnitude of the steady-state vacancy concentration during implantation, which is proportional to the dose rate multiplied by the density of elastic energy deposition, has only a small influence on the observed dose rate dependence. Moreover, for doses of the order of

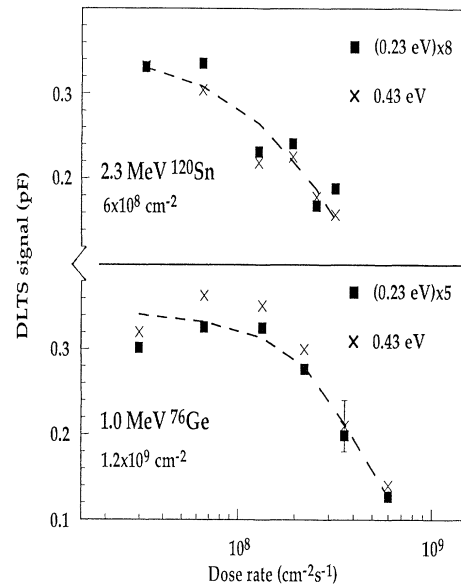


FIG. 2. Amplitudes of the levels at  $E_c - 0.23$  and  $E_c - 0.43$  eV as a function of dose rate for 2.3 MeV  $^{120}\text{Sn}$  and 1.0 MeV  $^{76}\text{Ge}$  ions keeping the dose constant at  $6 \times 10^8$  and  $1.2 \times 10^9 \text{ cm}^{-2}$ , respectively. Error bar indicates a relative accuracy of  $\pm 15\%$  and is given by the accuracy of the dosimetry.

$10^7 - 10^9 \text{ cm}^{-2}$ , the mean distance between adjacent ion tracks is in the range of 3 to  $0.3 \mu\text{m}$ . Hence, even if lateral straggling and vacancy diffusion [15] are taken into account, vacancy overlap between adjacent ion tracks during implantation is small for the low doses used in this work. Thus, vacancy clustering at high dose rates at the expense of formation of low order defects such as  $V_2$ , VO, and VP is anticipated to play a minor role. In addition, multivacancy complexes are electrically active because of their dangling Si bond character [16] but the two DLTS spectra in Fig. 1 are very similar in shape and no new levels occur at high dose rates. In this context it should also be pointed out that “ordinary” dynamic annealing is more pronounced in the regions containing isolated defects than in those regions where amorphous zones and extended defects are produced [5]. Thus, a qualitative comparison between the dynamic annealing results obtained at high doses ( $\geq 10^{12} \text{ cm}^{-2}$ ) by ion backscattering-channeling techniques [5] and those observed in the present work at low doses ( $10^7 - 10^9 \text{ cm}^{-2}$ ) may be regarded as relevant, although DLTS is only monitoring electrically active defects such as  $V_2$ . On the other hand,  $V_2$  is also observed by ion backscattering-channeling techniques at high enough concentrations [17].

Ionization-induced defect diffusion and annealing is known to occur in silicon [18], and this effect is anticipated to become more important at high dose rates because of a higher instantaneous concentration of electron-hole pairs (EHP). Results from *n*-type Si samples [19] implanted with  $^{11}\text{B}$ ,  $^{12}\text{C}$ ,  $^{16}\text{O}$ ,  $^{28}\text{Si}$ , and  $^{74}\text{Ge}$  ions using en-

ergies between 0.38 and 8.0 MeV reveal, however, a close proportionality between the peak concentration of the  $E_c - 0.43$  eV level and the number of vacancies per ion per  $\text{\AA}$  despite a variation in the production rate of EHP of  $\sim 10^{17}$  to  $\sim 10^{19} \text{ cm}^{-3}\text{s}^{-1}$ . In this work the production rate of EHP is in the range  $2 \times 10^{17} - 5 \times 10^{18} \text{ cm}^{-3} \text{ s}^{-1}$ , and ionization-induced annealing is not expected to influence the result shown in Fig. 2.

We favor a model where the decrease in defect production at high dose rates is due to rapidly diffusing silicon self-interstitials which overlap and annihilate vacancies created in adjacent ion tracks [7]. This annihilation is enhanced when the ion tracks occur sufficiently close in time and space. At low dose rates the vacancies created within an individual ion collision cascade have time to diffuse and form more stable defects (such as  $V_2$ ) before any interaction with later ion tracks. As a result, the concentration of simple vacancies becomes diluted and annihilation with interstitials from later ion tracks is small. However, at high dose rates, the vacancies created by one ion are still confined to a small volume when interstitials from later ions overlap, and the driving force for enhanced annihilation increases. In this context it must be pointed out that efficient annihilation also takes place between intracascade vacancies and interstitials. This occurs independently of dose rate, and the total concentration of electrically active vacancy-related defects after intracascade recombination and subsequent migration to form stable complexes amounts to less than 10% of the initial vacancy concentration [19].

Figure 3 shows that the concentration versus depth profiles of the  $E_c - 0.43$  eV level after high and low dose rate Ge implantations are identical in shape and only differ by a multiplying factor. Thus, within the experi-

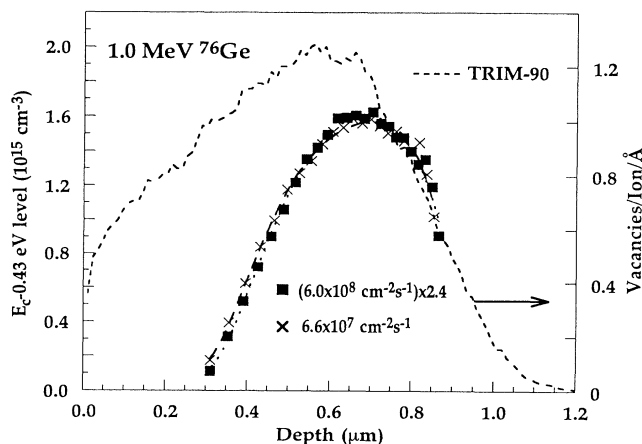


FIG. 3. Concentration versus depth profiles for the  $E_c - 0.43$  eV level in two samples implanted with 1.0 MeV  $^{76}\text{Ge}$  ions using dose rates of  $6.6 \times 10^7$  and  $6.0 \times 10^8 \text{ cm}^{-2}\text{s}^{-1}$ . The dose was kept constant at  $1.2 \times 10^9 \text{ cm}^{-2}$ . In the TRIM calculations 2800 runs (ions) were undertaken, and a displacement energy of 13 eV was assumed.

mental accuracy the relative importance of enhanced annihilation is constant as a function of depth. The experimental profiles in Fig. 3 are considerably narrower in shape with a much smaller tail towards the surface than the vacancy distribution calculated by TRIM (transport of ions in matter [20], version 90). As discussed in detail by Jagadish *et al.* [14,21], narrow profiles of  $V_2$  and VO centers are obtained if they are located close enough to the surface (depth of damage peak  $\leq 3 \mu\text{m}$ ). This is most likely caused by a surface-enhanced annihilation of migrating vacancies. The driving force for interstitials from adjacent ions to overlap is, however, primarily determined by the vacancy distribution after recombination with intracascade interstitials but before subsequent vacancy migration. The shape of this initial distribution is expected to resemble that of the TRIM profile, and a relatively constant rate of annihilation due to overlapping interstitials is anticipated in the depth range studied. Further support for this interpretation is given by the data in Fig. 4 showing an increase in the peak concentration of the  $E_c - 0.43$  eV level by almost a factor of 2 as the implantation temperature is raised from 95 to 304 K for 8.0 MeV  $^{120}\text{Sn}$  ions with a dose of  $\sim 5 \times 10^7 \text{ cm}^{-2}$ . This “reverse” temperature dependence of the defect production is attributed to a more stable distribution of simple vacancies at low temperatures because of a decreasing vacancy diffusion. The vacancies are confined to a small volume for a longer time, leading to an increased annihilation rate with interstitials from adjacent ions before the vacancies migrate to form stable defects.

In order to make a relative comparison with the experimental data in Fig. 4, we have utilized a model analogous

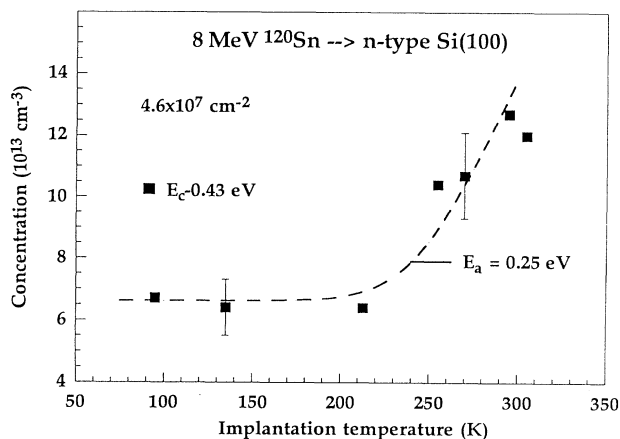


FIG. 4. Peak concentration of the  $E_c - 0.43$  eV level as a function of sample temperature during implantation with 8.0 MeV  $^{120}\text{Sn}$  ions. The dose and dose rate are held constant at  $4.6 \times 10^7 \text{ cm}^{-2}$  and  $1.5 \times 10^7 \text{ cm}^{-2}\text{s}^{-1}$ , respectively. A relative comparison is made with calculations using a model described in the text and assuming a migration energy of 0.25 eV for vacancy diffusion. Error bars indicate a relative accuracy of  $\pm 15\%$  and are given by the accuracy of the dosimetry.

to that in Ref. [7], where vacancies and interstitials are allowed to diffuse in one dimension perpendicular to the direction of ion incidence. As a first approximation, we have assumed a Gaussian vacancy distribution and only considered the peak value when estimating the relative temperature dependence of the annihilation rate with overlapping interstitials. A good fit to our data is obtained with an activation energy  $E_a$  of  $0.25 \pm 0.10$  eV for vacancy diffusion, leading to a decrease in the vacancy peak concentration and thereby a reduction in the rate of recombination with overlapping interstitials. The accuracy of the extracted  $E_a$  value is poor but  $E_a$  is in the range anticipated for vacancy migration ( $\sim 0.3$  eV for the neutral and  $\sim 0.18$  eV for the singly negative charge state [22]), and these promising results have stimulated a detailed study for a more precise determination of  $E_a$  and the reaction kinetics [23].

Moreover, using techniques other than DLTS, work is also in progress to reveal the dose dependence of the reverse temperature and dose rate effect observed in this study [24]. At high enough doses the concentration of defects in the silicon lattice becomes so large that only a minor interaction is anticipated between vacancies and interstitials generated in ion tracks that occur close in time. In particular, this holds for low dose rates where the distance between such tracks is large, and an interaction may be readily suppressed by other defects.

In summary, a reverse temperature and dose rate dependence is observed for the production of stable vacancy-related point defects in silicon implanted with low doses ( $10^7$ – $10^9$  cm $^{-2}$ ) of MeV  $^{76}\text{Ge}$  and  $^{120}\text{Sn}$  ions. This effect is attributed to rapidly diffusing silicon self-interstitials which overlap and annihilate vacancies created in adjacent ion tracks. The annihilation is enhanced at high dose rates and/or low temperatures where the vacancies generated by individual ion cascades are still confined to a small volume when interstitials from later ion tracks overlap. At low dose rates and/or high temperatures, the vacancies created by individual ion tracks have started to migrate and form more stable defects (such as  $V_2$ ) before later ions arrive. Thus, the vacancy concentration becomes diluted and annihilation with interstitials from later ions is small.

Fruitful discussions with Dr. A. Hallén and the experimental assistance by Dr. N. Hauser in preparing the Schottky barrier contacts are highly appreciated.

\*Permanent address: Royal Institute of Technology, Solid State Electronics, P.O. Box 1298, S-164 28 Kista-Stockholm, Sweden.

- [1] F. F. Morehead and B. L. Crowder, *Rad. Effects* **6**, 27 (1970).
- [2] F. Eisen and B. Welch, *Rad. Effects* **7**, 143 (1971).
- [3] G. Holmén, A. Burén, and P. Högborg, *Rad. Effects* **24**, 51 (1975).
- [4] J. S. Williams, M. W. Austin, and H. B. Harrison, in *Thin Film Interfaces and Interactions*, edited by J. E. E. Baglin and J. M. Poate (Electrochemical Society, Princeton, 1980), p. 137.
- [5] See, e.g., J. M. Poate and J. S. Williams, in *Ion Implantation and Beam Processing*, edited by J. S. Williams and J. M. Poate (Academic, Sydney, 1984), p. 13.
- [6] T. E. Haynes and O. W. Holland, *Appl. Phys. Lett.* **59**, 452 (1991).
- [7] A. Hallén, D. Fenyö, B. U. R. Sundqvist, R. E. Johnson, and B. G. Svensson, *J. Appl. Phys.* **70**, 3025 (1991).
- [8] B. G. Svensson, K.-H. Rydén, and B. M. S. Lewerentz, *J. Appl. Phys.* **66**, 1699 (1989).
- [9] G. D. Watkins and J. W. Corbett, *Phys. Rev.* **121**, 1001 (1961); J. W. Corbett, G. D. Watkins, R. M. Chrenko, and R. S. McDonald, *ibid.* **121**, 1015 (1961).
- [10] A. O. Eswarayee and E. Sun, *J. Appl. Phys.* **47**, 3776 (1976).
- [11] L. C. Kimerling, in *Radiation Effects in Semiconductors—1976*, edited by N. B. Urli and J. W. Corbett, IOP Conf. Proc. No. 31 (Institute of Physics, Bristol, 1977), p. 221.
- [12] S. D. Brotherton and P. Bradley, *J. Appl. Phys.* **53**, 5720 (1982).
- [13] B. G. Svensson and M. Willander, *J. Appl. Phys.* **62**, 2758 (1987).
- [14] C. Jagadish, B. G. Svensson, and N. Hauser, *Semicond. Sci. Technol.* **8**, 481 (1993).
- [15] G. D. Watkins, in *Radiation Effects in Semiconductors*, edited by F. L. Vook (Plenum, New York, 1968), p. 67; J. A. van Vechten, *Phys. Rev. B* **10**, 1482 (1974).
- [16] See, e.g., Y.-H. Lee and J. W. Corbett, *Phys. Rev. B* **13**, 2653 (1976), and references therein.
- [17] O. W. Holland, M. K. El-Ghor, and C. W. White, *Appl. Phys. Lett.* **53**, 1282 (1988).
- [18] J. W. Corbett and J. C. Bourgoin, in *Point Defects in Solids*, edited by J. H. Crawford and L. M. Slifkin (Plenum, New York, 1975), p. 1.
- [19] B. G. Svensson, C. Jagadish, and J. S. Williams, *Nucl. Instrum. Methods Phys. Res., Sect. B* **80/81**, 583 (1993).
- [20] J. P. Biersack and L. G. Haggmark, *Nucl. Instrum. Methods* **174**, 257 (1980).
- [21] C. Jagadish, B. G. Svensson, N. Hauser, and J. S. Williams, *Thin Solid Films* **222**, 173 (1992).
- [22] P. M. Fahey, P. G. Griffin, and J. D. Plummer, *Rev. Mod. Phys.* **61**, 289 (1989).
- [23] C. Jagadish, B. G. Svensson, and J. S. Williams (to be published).
- [24] P. Kringhøj, C. Jagadish, L. Josyula, and B. G. Svensson (to be published).